Cellular Physiology and Biochemistry

Cell Physiol Biochem 2018;45:1410-1422
DOI: 10.1159/000487567
Published online: February 20, 2017
Accepted: January 09, 2018

Original Paper

Effects of MicroRNA-206 on Osteosarcoma Cell Proliferation, Apoptosis, Migration and Invasion by Targeting ANXA2 Through the AKT Signaling Pathway

Bao-Long Pan[a] Zong-Wu Tong[b] Ling Wu[c] Li Pan[a] Jun-E Li[a]
You-Guang Huang[d] Shu-De Li[e] Shi-Xun Du[a] Xu-Dong Li[a]

[a]Department of Laboratory, People's Hospital of Yuxi City, Yuxi, [b]Department of nephrology, People's Hospital of Yuxi City, Yuxi, [c]Department of Quality Control, Central blood station of Yuxi city, Yuxi, [d]Tumor Markers Research Center, Tumor Institute of Yunnan Province, The Third Affiliated Hospital of Kunming Medical University, Kunming, [e]Department of Biochemistry and Molecular Biology, School of Basic Medical Science, Kunming Medical University, Kunming, P.R. China

Key Words
MicroRNA-206 • ANXA2 • AKT signaling pathway • Osteosarcoma • Proliferation • Invasion

Abstract
Background/Aims: This study aimed to investigate the mechanism by which microRNA-206 (miR-206) affects the proliferation, apoptosis, migration and invasion of osteosarcoma (OS) cells by targeting ANXA2 via the AKT signaling pathway. ***Methods:*** A total of 132 OS tissues and 120 osteochondroma tissues were examined in this study. The targeting relationship between miR-206 and ANXA2 was verified with a dual-luciferase reporter assay. The miR-206 expression and ANXA2, AKT, PARP, FASN, Survivin, Bax, Mcl-1 and Bcl-1 mRNA and protein expression in the above two groups were examined by qRT-PCR and western blotting. The cultured OS cells were divided into 6 groups: a blank group, negative control (NC) group, miR-206 mimic group, miR-206 inhibitor group, si-ANXA2 group and miR-206 inhibitor + si-ANXA2 group. Cell cycle and apoptosis were assessed by flow cytometry, cell migration was examined with a wound-healing assay, and cell invasion was assessed with a Transwell assay. Pearson correlation analysis was used to determine the correlation between ANXA2 mRNA expression and miR-206 expression in OS. ***Results:*** OS tissues exhibited increased mRNA and protein expression of ANXA2, AKT, PARP, FASN, Survivin, Mcl-1 and Bcl-2; decreased miR-206 expression; and decreased Bax mRNA and protein expression. ANXA2 mRNA expression was strongly negatively correlated with miR-206 expression in OS. ANXA2 was found to be a miR-206 target gene. In the miR-206 mimic group and the si-ANXA2 group, the mRNA and protein expression of ANXA2, AKT, PARP, FASN, Survivin, Mcl-1 and Bcl-1 decreased

B.-L. Pan and Z.-W. Ting contributed equally to this work.

You-Guang Huang
and Shu-De Li

Tumor Markers Research Center, Tumor Institute of Yunnan Province, The Third Affiliated Hospitalof Kunming Medical University, 519 Kunzhou Road, Kunming 650118, Yunan Province (China); E-Mail huangyouguang2008@126.com, shudeli006@vip.sina.com

markedly, cell proliferation was inhibited, apoptosis was promoted, higher cell growth in G1 phase and decreased growth in S phase was detected, and decreased cell migration and invasion were observed compared with those in the blank group. ***Conclusion:*** The current results demonstrate that miR-206 overexpression inhibits OS cell proliferation, migration and invasion and promotes apoptosis through targeting ANXA2 by blocking the AKT signaling pathway.

Introduction

Osteosarcoma (OS) is the most common malignant bone tumor, has a high incidence and mortality in children and adolescents and exhibits high destructive and metastatic potential [1]. However, the precise etiology of OS and a rational treatment approach remain elusive [2]. The commonly used therapeutic strategies include preoperative chemotherapy or radiotherapy, surgical resection of all known disease or metastatic tissues and postoperative management [3]. However, these treatments have failed to promote complete recovery because of chemoresistance, and patient prognosis is often poor; furthermore, secondary occurrence of the disease is high [4]. Fortunately, with the recently expanding body of research, increasing evidence indicates that this disease is a differentiation disease arising from genetic and epigenetic differentiation of mesenchymal stem cells into osteoblasts [5]. It is distinct from the identified role of other chromosome aberrations in OS, such as 6P12 and cMYC, and little is known about the role that microRNAs (miRNAs) may play in curing this malignant cancer [6].

miRNAs are a class of small, noncoding, single-stranded RNA molecules that are approximately 18-25 nucleotides in length, and they play critical roles in regulating gene expression and in biological processes, such as proliferation, differentiation and apoptosis of tumor cells [7]. In recent years, miRNA molecules have been found to be an important part of cancer diagnosis and prognosis, and they are potential biomarkers and therapeutic targets for drug discovery [8]. miR-206, a member of the tumor suppressive miRNA family, has been found to be down-regulated in human malignancies relevant to tumor progression, including human OS [9]. Annexin A2 (ANXA2), a calcium- and phospholipid-dependent protein, is distributed throughout the cell surface and could be a biomarker for certain tumors because ANXA2 deregulation and upregulation are associated with cancers from initiation to metastasis [10]. AKT/Protein kinase B (AKT/PKB) is a family that includes three homologous members and plays a remarkable role in cell survival and protein synthesis; family members are classified as serine/threonine protein kinases [11]. A previous study has suggested the possibility that miRNAs, such as miR-93, target certain genes and take part in regulating the AKT/PKB signaling pathway [12]. In the present study, we explore and elaborate on the role of miR-206 in regulating the proliferation and invasion of OS cells by targeting ANXA2 via the AKT signaling pathway.

Materials and Methods

Study Subjects

Altogether, 132 OS tumor tissue samples derived from 132 OS patients were collected from September 2011 to September 2016. Among the 132 OS patients, 74 were males and 58 were females, with ages ranging from 9 to 53 years (mean age: 27.21 ± 9.34 years old). Overall, 120 amputees were selected to obtain osteochondroma (a benign bone lesion) tumor tissue samples; they included 69 males and 51 females, whose ages ranged from 8-58 and whose mean age was 27.93 ± 10.87. Both groups met the following inclusion criteria: traditional OS was confirmed by clinical, imaging and case diagnosis; tumors were located only in limbs, with no metastasis before diagnosis; patients underwent standard diagnostic procedures; and none of the patients were treated with radiotherapy or chemotherapy. The following exclusion criteria were noted: secondary symptoms; diagnostic procedures not complied with; other therioma history on

record; and metastasis occurring before diagnosis. Each sample was preserved at -80°C. This study was conducted in accordance with the Declaration of Helsinki and received approval from the Ethical Committee of Yunnan Cancer Hospital & The Affiliated Hospital of Kunming Medical University & Yunnan Cancer Center. The above samples were collected from patients who provided informed consent.

Hematoxylin and eosin (HE) staining

All samples in the two groups were fixed with 10% neutral buffered formalin for 16-18 h (5-7 days of decalcification was necessary for bone tissue), dehydrated by gradient alcohol, hyalinized in xylene, dipped in wax, embedded in paraffin and subsequently continuously sectioned at a thickness of 5 μm. Next, the sections were spread out at 45°C, roasted at 60°C for 1 h, and dewaxed by xylene. Subsequently, gradient HE staining (Beijing Solarbio Science & Technology Co., Ltd., Beijing, China) was performed after hydration. After secondary dehydration and vitrification and sealing with neutral balsam, the pathological changes in these sections were observed under an optical microscope (CX31-LV320, Olympus Optical Co., Beijing, China).

Immunocytochemistry

OS and osteochondroma tissues were embedded in paraffin, and 3- to 4-μm sections were prepared. The sections were placed in 3% H_2O_2 before gradient dewaxing and hydration for 20 min at room temperature to block endogenous peroxidase. Antigen repair was underway after incubation in an 80% power microwave for 5 min. Rabbit anti-mouse Annexin A2 (ANXA2) (ab178677, Abcam Inc., Cambridge, MA, USA) monoclonal antibody (1:1000) was incubated with sections at 4°C overnight, and biotinylated goat anti-mouse IgG secondary antibody (1:1000, ab6789, Abcam Inc., Cambridge, MA, USA) was added and incubated with sections at 37°C for 30 min. Then, secondary staining with hematoxylin (No: Co105, Beyotime Biotechnology Co., Shanghai, China) was performed for 30 s, and the tissues were developed with diaminobenzidine (DAB) (No: P0202, Beyotime Biotechnology Co., Shanghai, China). The sections were dehydrated with hydrochloric acid and alcohol until vitrification, sealed with balsam, and subsequently observed and photographed under a microscope (CX31-LV320, Olympus Optical Co., Beijing, China). Two positive and negative results were presented: brownish yellow in the cytoplasm and cytomembrane indicated positive staining, and otherwise indicated negative staining. The positive protein expression rate was calculated as follows: five 200× fields were randomly selected for detection, and the ratio of the positive cells was calculated. The experiment was performed 3 times.

Quantitative real-time polymerase chain reaction (qRT-PCR)

Approximately 100 mg of frozen tissue was placed into a glass homogenizer to obtain total homogenate. A Trizol™ kit (No: 16096020, Thermo Fisher Scientific Inc., Waltham, MA, USA) was adopted to obtain total RNA using a two-step method. Primers were designed by Premier 5 and Oligo 6 and are shown in Table 1; Takara Co. performed the synthesis. Subsequently, 10 μL of RNA was diluted 1/20 times in RNase-free ultrapure water to test the concentration and purity by recording the absorption values at 260 and 280 nm via ultraviolet (UV) spectrophotometry. The total RNA value was 1.25/optical density (OD) 260 (μL). Altogether, 5 μL of the kit reagent, 5 μL of total RNA and 10 μL of RNase-free H_2O were added to an Eppendorf tube, centrifugally mixed and reacted in qPCR. The following reaction conditions were used: 37°C for 15 min and 85°C for 5 s; the reaction was stopped at 4°C; and cDNA was obtained and preserved at -20°C. An ABI 7500 quantitative PCR

Table 1. Primer sequences for PCR. Notes: PCR, polymerase chain reaction; F, forward; R, reverse; miR-206, microRNA-206; ANXA2, Annexin A2; PARP, poly ADP-ribose polymerase; FASN, fatty acid synthase; Bax, Bcl-2 associated X protein; Mcl-1, myeloid cell leukemia 1; Bcl-2, B cell lymphoma 2; GAPDH, glyceraldehyde-3-phosphate dehydrogenase

Gene	Primer sequence
miR-206	F: 5'-CAGATCCGATTGGAATGTAAGG-3'
	R: 5'-TATGCTTGTTCTCGTCTCTGTGTC-3'
ANXA2	F: 5'-TGAGCGGGATGCTTTGAAC-3'
	R: 5'-ATCCTGTCTCTGTGCATTGCTG-3'
AKT	F: 5'-CATCACATCTGGTTTCCTTGG-3'
	R: 5'-AACTGGAAATGTAATTTTGGG-3'
PARP	F: 5'-ATGAAGTGAAGGCCATGATTG-3'
	R: 5'-TCCTTTAACGATGTCCACCAG-3'
FASN	F: 5'-ATTCCGGGCCAAGTTCTAC-3'
	R: 5'-GCGCATGTACAGCTCGTG-3'
Survivin	F: 5'-GCGAAGCTTACCATGGGTGCCCCGACGTTG-3'
	R: 5'-CGCGGATCCATATCCATGGCAGCCAGCTG-3'
Bax	F: 5'-AGCTCTGAGCAGATCATGAAGAC-3'
	R: 5'-AGTTGAAGTTGCCGTCAGAAAAC-3'
Mcl-1	F: 5'-CAACGATTTCACATCGTCTTCGT-3'
	R: 5'-TTGATGTCCAGTTTCCGAAGCATGCCT-3'
Bcl-2	F: 5'-CGTCATAACTAAAGACACCCC-3'
	R: 5'-TTCATCTCCAGTATCCCACTC-3'
GAPDH	F: 5'-TGGTGAAGGTCGGTGTGAAC-3'
	R: 5'-GCTCCTGGAAGATGGTGATGG-3'
U6	F: 5'-TTTGAATTCCCCCAGTGGAAAGACGCGCAG-3'
	R: 5'-TGGGGATCCGGTGTTTCGTCCTTTCCACAA-3'

instrument (ABI 7500, ABI Company, Oyster Bay, NY, USA) was used in this experiment with the following conditions: SYBRGreen fluorescent dye (No: RR091A, Takara Holdings Inc., Kyoto, Japan) was applied for pre-denaturation at 95°C for 10 min, followed by 40 cycles of denaturation at 95°C for 10 s, annealing at 60°C for 20 s and elongation at 72°C for 34 s. U6 was used as the internal reference for miR-206 expression, and glyceraldehyde-3-phosphate dehydrogenase (GAPDH) was used as the internal reference for ANXA2, AKT, poly ADP-ribose polymerase (PARP), fatty acid synthase (FASN), Survivin, Bcl-2 Associated X protein (Bax), myeloid cell leukemia 1 (Mcl-1) and B cell lymphoma 2 (Bcl-2) expression. The relative quantitative method and $2^{-\triangle\triangle Ct}$ method [13] were adopted to calculate the relative transcription levels of target genes (miR-206, ANXA2, AKT, PARP, FASN, Survivin, Bax, Mcl-1 and Bcl-2): $\Delta\Delta Ct = \Delta Ct_{RAgroup} - \Delta Ct_{normal\ group,}$ $\Delta Ct = Ct_{target\ gene} - Ct_{internal\ reference.}$ The gene expression levels in each group were compared. The experiment was repeated 3 times and was suitable for cell experiments.

Western blotting

The obtained OS and osteochondroma tumor tissues were added to liquid nitrogen and ground into a thin powder, which was subsequently centrifuged at 13000 r/min and 4°C for 15 min after the addition of lysate (No: C0481, Sigma-Aldrich Chemical Co., St Louis MO, USA), and the supernatant was stored for later experiments. Next, the protein concentration in the samples was assessed with a bicinchoninic acid (BCA) assay and adjusted to be consistent with the loading quantity by removing ionized water. Then, 10% separation and stacking gels for sodium dodecyl sulfate (SDS) electrophoresis were generated. After mixing the sample and loading buffer, the mixture was boiled at 100°C for 5 min, and the equivalent sample amounts were electrophoretically separated using pipettes after an ice-bath and centrifugation. Subsequently, the protein on the gel was transferred onto a nitrocellulose membrane, followed by blocking with 5% skimmed milk powder at 4°C overnight. Rabbit anti-human antibodies targeting ANXA2 (1:1000, ab178677, Abcam Inc., Cambridge, MA, USA), AKT (1:500, ab8805, Abcam Inc., Cambridge, MA, USA), PARP (1:2000, ab32064, Abcam Inc., Cambridge, MA, USA), FASN (1:1000, ab22759, Abcam Inc., Cambridge, MA, USA), Survivin (1:5000, ab76424, Abcam Inc., Cambridge, MA, USA), Bax (1:1000, ab32503, Abcam Inc., Cambridge, MA, USA), Mcl-1 (1:1000, ab32087, Abcam Inc., Cambridge, MA, USA), Bcl-2 (1:1000, ab32124, Abcam Inc., Cambridge, MA, USA) and GAPDH (1:2000, ab8245, Abcam Inc., Cambridge, MA, USA; internal reference) proteins were added, incubated with the membranes for 1 h, and washed 3 times with phosphate-buffered saline (PBS) (5 min each time) at room temperature. Following the addition of goat anti-rabbit IgG secondary antibody (1:1000, Wuhan Boster Biological Technology Co., LTD., Hubei, China), the sample was reacted at room temperature for 1 h, followed by 3 washes with PBS (5 min each time). The membrane was immersed in electrochemiluminescence (ECL) reaction solution (Pierce Manufacturing Inc. Appleton, WI, USA) for 1 min at room temperature and was then covered with preservative film to remove the liquid. The results were acquired via X-ray detection. Taking GAPDH as an internal reference, the ratio of the gray values between the target and reference bands was considered the comparative expression of proteins. The experiment was repeated 3 times (appropriate for the cell experiment).

Verification of a targeting relationship between miR-206 and ANXA2

Target gene analysis was conducted to analyze miR-206, and its targeting relationship with ANXA2 was predicted using the bioinformatics prediction website microRNA.org. The artificial ANXA-3'UTR gene segment was introduced into a pMIR-reporter (Promega Corporation, Madison, WI, USA) via the endonuclease cleavage sites SalI and BglII. Complementary sequence mutant sites of the seed sequence were designed at ANXA2 wild type, and the target segment was inserted into the pMIR-reporter plasmid with T4 DNA ligase via restriction endonucleases. The PRL-TK carrier expressing Renilla luciferase (Takara Biotechnology Ltd., Dalian, China) was taken as the internal reference to regulate the cell quantity and differences in transfection efficiency. miR-206 mimic and negative reference were co-transfected into OS cells with the luciferase reporter, and after 48 h, the cells were collected and disrupted. The Dual-Luciferase Reporter Assay System (Promega Corporation, Madison, WI, USA) was used to test the activity of luciferase. The experiment was repeated 3 times.

Cell transfection

The human OS cell line MG-63 (Cell Resource Center, IBMS, CAMS/PUMC, Beijing, China) was cultured in Dulbecco's modified Eagle's medium (DMEM) (Gibco Co., Grand Island, NY, USA) containing 10% fetal

bovine serum, seeded onto a 6-well culture plate at a density of 1 × 10^5 cells in each well and then cultivated in an incubator with a saturated humidity of 5% CO_2 at 37°C. At 80 - 90% confluence, cells were passaged in DMEM containing 10% fetal bovine serum.

Table 2. Transfection Sequences. Notes: miR-206, microRNA-206; ANXA2, Annexin A2

Group	Primer sequence
miR-206 mimic	5′-TGGAATGTAAGGAAGTGTGTGG-3′
miR-206 inhibitor	5′-CCACACACUUCCUUACAUUCCA-3′
si-ANXA	5′-GAACUUGCAUCAGCACUGATT-3′

Extracted human OS cells in logarithmic phase were transfected and assigned to 6 groups: a blank group (no transfection), negative control group (transfected with NC sequence in transfection kit), miR-206 mimic group (transfected with miR-206 mimic sequence), miR-206 inhibitor group (transfected with miR-206 inhibiting sequence), si-ANXA2 group (transfected with siRNA sequence of ANXA2) and miR-206 inhibitor + si-ANXA2 group (co-transfected with miR-206 inhibitor and siRNA sequence of ANXA2). All transfected sequences (Table 2) were synthesized by Shanghai Sangon Biotech Co. Ltd. (Shanghai, China). The following procedures were conducted for cell transfection: cell passage was addressed before the day of transfection, and cells were inoculated onto a 6-well plate with 1 × 10^5 cells in each well until 70-80% confluence was reached. Cell transfection was performed with a Lipofectamine® 2000 kit (11668019, Invitrogen Inc., Carlsbad, CA, USA) as indicated. Altogether, 250 μL of DMEM containing no serum was used to dilute 100 pmol of the above groups, except for the blank group (the final concentration was 50 nM); the same medium was used to dilute 5 μL of Lipofectamine® 2000, followed by incubation for 5 min at room temperature after mixing well. After complete mixture of the above samples, a 20-min incubation at room temperature was conducted prior to addition of the mixed solutions to the culture wells. Following the transfection, the cells were cultured in the incubator with 5% CO_2 at 37°C for 6-8 h. Finally, the complete culture medium was cultured for another 24-48 h for a later experiment.

Cell counting kit-8 (CCK-8) assay

Transfected human OS cells were seeded onto a 96-well plate, and 100 μL of culture medium was added. The density of the cells was adjusted to 2 × 10^3 cells/mL. The plate was incubated at 37°C for culture, and cell activity was recorded after 24, 48 and 72 h. After adding 10 μL of CCK-8 kit reagent (C0037, Beyotime Biotechnology Co., Shanghai, China) and incubation at 37°C for 2 h, the OD value was recorded at 450 nm/630 nm using a microplate reader (Multiskan FC, Thermo Fisher Scientific Inc., NY, USA). Three parallel wells were set in each group, and the mean value was calculated. A cell activity graph was drawn, with the x-axis referring to time and the y-axis representing the OD value. The experiment was repeated 3 times.

Flow cytometry (FCM) assay

After 48 h of transfection, the culture medium was removed, and the cells were washed once with PBS solution. After digestion with 0.25% trypsin solution, the cells were observed under a microscope until they became round. Subsequently, serum culture medium was added to terminate digestion. A cell suspension was produced after isolating cells from the cytoderm and was centrifuged at 1000 r/min for 5 min, with the supernatant subsequently removed. After two washes with PBS, the cells were fixed with 70% pre-chilled ethanol for 30 min and collected by centrifugation. After washing with PBS, the cells were stained with 1% propidium iodide (PI) containing RNA enzyme for 30 min. Then, the PI was rinsed off twice via PBS washes. The volume was adjusted to 1 mL with PBS. Finally, the cell cycle distribution was assessed by putting samples into a BD-Aria FACSCalibur flow cytometer (FACSCalibur; Beckman Coulter, Inc., Chaska, MN, USA) (there were 3 samples in each group, and the experiments were performed 3 times).

At 48 h after transfection, the cells were digested by pancreatin with no ethylenediaminetetraacetic acid (EDTA), collected into flow tubes and centrifuged; then, the supernatant was abandoned. After 3 washes with chilled PBS, the cells were centrifuged, and the supernatant was abandoned again. Following the instructions of the Annexin-V-fluorescein isothiocyanate (Annexin-V-FITC) cell apoptosis kit (C1065, Beyotime Biotechnology Co., Shanghai, China), Annexin-V-FITC, PI and hydroxyethyl piperazine ethanesulfonic acid (HEPES) buffer solutions were used to prepare the Annexin-V-FITC/PI staining solution at a ratio of 1: 2: 50. Then, 1 × 10^6 cells were resuspended in every 100 μL of staining solution. After being well mixed, the cells were incubated for 15 min at room temperature and later mixed again following the

addition of 1 mL of HEPES. A 488-nm wavelength was used for excitation, with a 525 and 620 nm bandpass filter, to detect cell apoptosis by measuring FITC and PI fluorescence.

Wound-healing assay

Transfected cells were seeded onto a 6-well plate with 5×10^5 cells per well. When the cell confluence reached approximately 90%, a thin wound was created along the center of each well with a sterile pipette tip. After the floating cells were washed out with PBS, the cells were cultured in serum-free medium for 0.5-1 h until cell recovery occurred. Taking the precise moment of cell recovery as 0 h, images were acquired at 0 and 48 h. Finally, the cell migration distance was examined using Image-Pro Plus Analysis software (Media Cybernetics, Inc., Rockville, MD, USA). Three experiments were required to obtain an average value.

Transwell assay

Serum-free culture medium (1:3) was used to diluted Matrigel (No: 356234, Becton, Dickinson and Company, NJ, USA), which was incubated at 4°C overnight. Matrigel was added to the upper surface of the Transwell chamber, with 50 μL in each well, and equilibrated for 30 min in the incubator. A cell suspension of 1×10^5/mL was seeded onto the upper chamber, with serum-free medium in the bottom chamber. Subsequently, 10% FBS medium was added to the bottom chamber for the 24-h invasion assay. Cell invasion ability was measured as the number of cells passing through the chamber. The mean value was obtained via 3 experiments.

Statistical analysis

All data analyses were conducted using SPSS 21.0 (IBM Corp., Armonk, NY, USA). The results are expressed as the means ± standard deviation. Differences between two groups were compared by LSD-t, and differences between multiple groups were examined by variance analysis. Pearson correlation analysis was used to determine the correlation between ANXA2 mRNA expression and miR-206 expression in OS. $P < 0.05$ was considered statistically significant.

Results

Pathological changes in OS and osteochondroma tissues

Three layers were observed in osteochondroma tumor tissues, with fibrous tissue detected in the outer layer, cartilaginous tissue in the middle layer and bone formation in the internal layer, which indicated that the cells had been fully differentiated, with no variation. In contrast, OS cells in tissues were concentrated and presented marked nuclear atypia, and they were increased in both number and size, with more hyperchromatic nuclear grains resulting from increased nuclear chromatin. Notably, nuclear division was observed. A neoplastic bone and labyrinthine osteoid matrix appeared among atypical spindle cells with infiltrative growth (invading the surrounding bone tissues) (Fig. 1).

Immunohistochemical results of ANXA2 analysis in OS and osteochondroma tissues

The results suggested that ANXA2 was highly expressed in the cell membrane. The cell cytoplasm presented a brownish yellow color, and ANXA2 was somewhat distributed in the nucleus. Obviously more intense staining was present in OS tissues than in osteochondroma tissues, and the protein expression of ANXA2 in OS tissues (51.3%) was dramatically higher than that in osteochondroma tissue (17.8%) ($P < 0.05$) (Fig. 2).

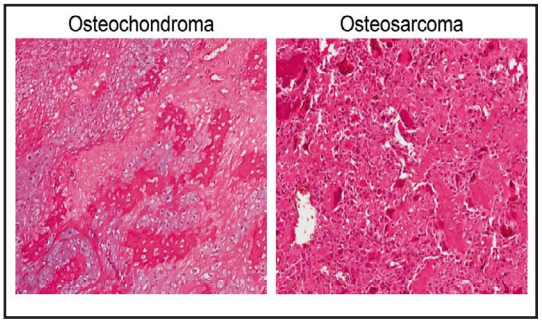

Fig. 1. Results of HE staining of OS and osteochondroma tissue samples (100 ×). Notes: OS, osteosarcoma; HE, hematoxylin and eosin.

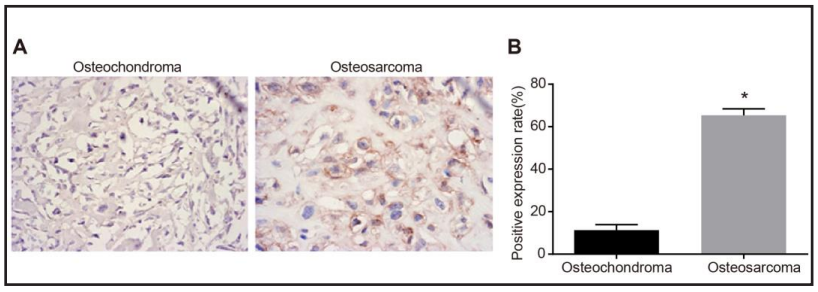

Fig. 2. Results of immunohistochemical analysis of ANXA2 protein expression in OS and osteochondroma tissue samples. Note: A, Immunohistochemical ANXA2 protein staining results in OS and osteochondroma tissue samples; B, Positive ANXA2 expression rate in OS and osteochondroma tissue samples; *, P<0.05 compared with the osteochondroma tissue samples. Note: ANXA2, Annexin A2; OS, osteosarcoma.

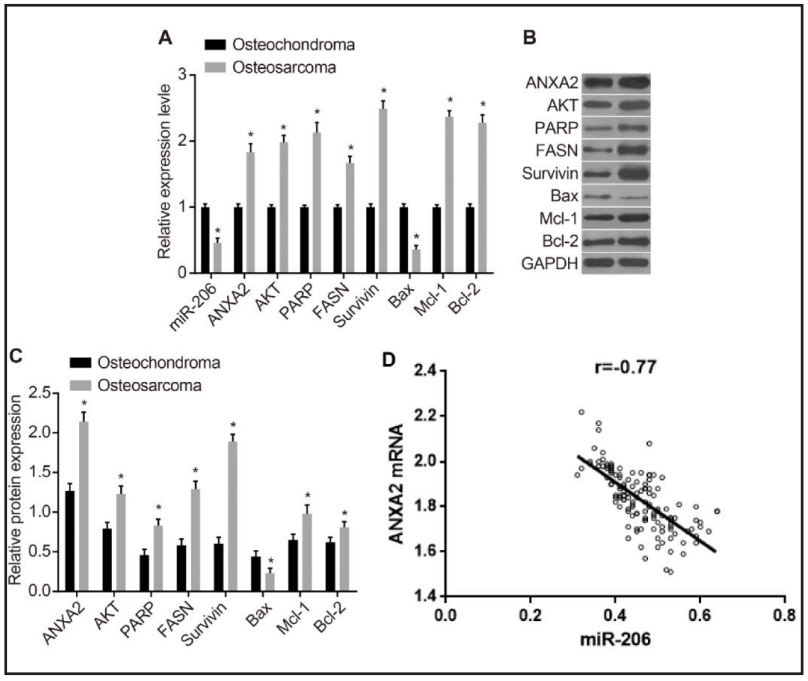

Fig. 3. miR-206 expression and mRNA and protein expression of ANXA2, AKT, PARP, FASN, Survivin, Bax, Mcl-1 and Bcl-2 in tissue samples. Note: A, miR-206 expression and mRNA expression of ANXA2, AKT, PARP, FASN, Survivin, Bax, Mcl-1 and Bcl-2 in the OS and osteochondroma tissue samples; B, western blotting images showing ANXA2, AKT, PARP, FASN, Survivin, Bax, Mcl-1 and Bcl-2 expression in OS and osteochondroma tissue samples; C, protein expression of ANXA2, AKT, PARP, FASN, Survivin, Bax, Mcl-1 and Bcl-2 in OS and osteochondroma tissue samples; D, negative correlation between ANXA2 mRNA expression and miR-206 expression; *, P<0.05 compared with the osteochondroma tissue samples. Note: OS, osteosarcoma; miR-206, microRNA-206; ANXA2, Annexin A2; PARP, poly ADP-ribose polymerase; FASN, fatty acid synthase; Bax, Bcl-2 associated X protein; Mcl-1, myeloid cell leukemia 1; Bcl-2, B cell lymphoma 2; GAPDH, glyceraldehyde-3-phosphate dehydrogenase.

miR-206 expression and mRNA and protein expression of ANXA2, AKT, PARP, FASN, Survivin, Mcl-1 and Bcl-2 in OS and osteochondroma tissues

As detected by qRT-PCR and western blotting (Fig. 3), ANXA2, AKT, PARP, FASN, Survivin, Mcl-1 and Bcl-2 were expressed at higher levels in OS tissues than in osteochondroma tissues; however, the mRNA and protein expression of Bax and miR-206 was significantly decreased (all $P < 0.05$). ANXA2 mRNA expression was strongly negatively correlated with miR-206 expression in OS ($P < 0.05$).

ANXA2 is the target gene of miR-206

The target site of miR-206 on ANXA2 was confirmed via an online prediction website. Fig. 4A shows the mRNA sequence of ANXA2 and the 3'-UTR sequence combined with miR-206. To verify whether miR-206 binding to the predicted site leads to changes in luciferase activity, wild-type and mutant sequences lacking the miR-206 combination sites in the ANXA2

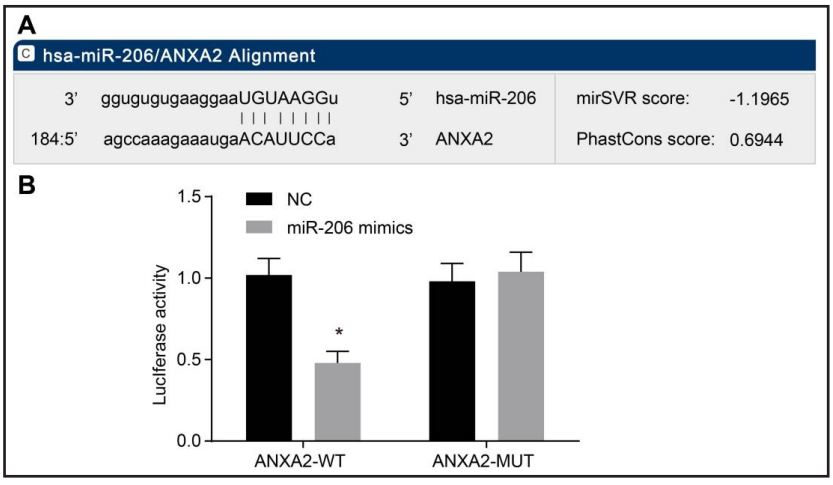

Fig. 4. miR-206 directly targets ANXA2. Note: A, prediction alignment of miR-206 and the ANXA2 3'UTR; B, detection of luciferase activity; *, P<0.05 compared with the NC group. Note: ANXA2, Annexin A2; NC, negative control; WT, wild type; MUT, mutant; NC, negative control; UTR, untranslated regions.

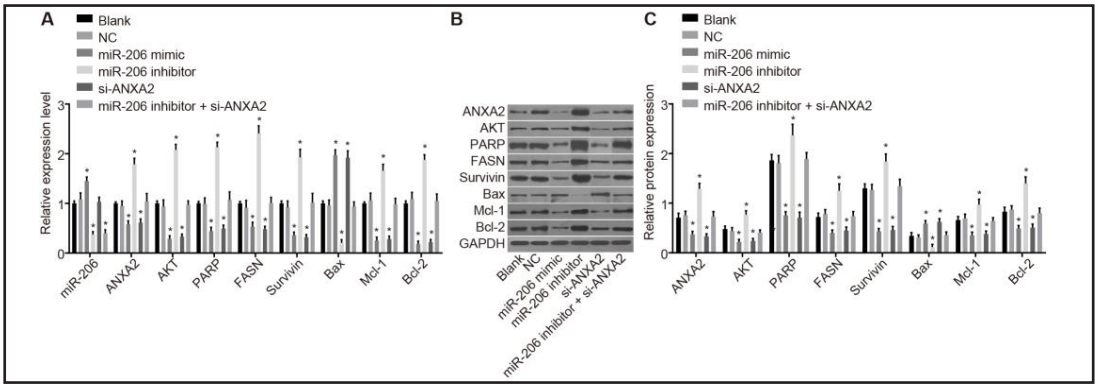

Fig. 5. miR-206 expression and mRNA and protein expression of ANXA2, AKT, PARP, FASN, Survivin, Bax, Mcl-1 and Bcl-2 in cell experiments. Note: A, mRNA expression in six groups; B, western blotting of protein expression in six groups; C, protein expression in cells from six groups; *, P<0.05 compared with the blank group. Note: miR-206, microRNA-206; ANXA2, Annexin A2; PARP, poly ADP-ribose polymerase; FASN, fatty acid synthase; Bax, Bcl-2 associated X protein; Mcl-1, myeloid cell leukemia 1; Bcl-2, B cell lymphoma 2; GAPDH, glyceraldehyde-3-phosphate dehydrogenase.

3'-UTR were inserted into a reporter plasmid. The miR-206 mimic and WT-miR-206/ANXA2 or MUT-miR-206/ANXA2 recombinant plasmids were co-transfected into OS cells, and the results showed that MUT-miR-206/ANXA2 had no significant effects on the luciferase activity, but the luciferase activity was markedly decreased in the WT-miR-206/ANXA2 group ($P < 0.05$) (Fig. 4B).

Comparison of miR-206, ANXA2, AKT, PARP, FASN, Survivin, Bax, Mcl-1 and Bcl-2 expression among six groups

Between the blank group and the NC group, the expression of miR-206, ANXA2, AKT, PARP, FASN, Survivin, Bax, Mcl-1 and Bcl-2 presented no significant difference (all $P > 0.05$). Compared with the blank group, miR-206 was more highly expressed in the miR-206 mimic group ($P < 0.05$), and miR-206 showed no statistically significant expression difference in the si-ANXA2 group ($P > 0.05$). However, the mRNA and protein expression of ANXA2, AKT, PAPP, FASN, Survivin, Mcl-1 and Bcl-2 was reduced in the miR-206 mimic

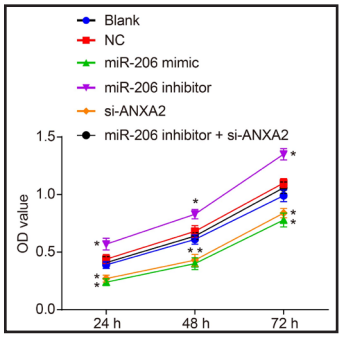

Fig. 6. Cell growth at 24, 48 and 72 h in the six groups. Note: *, P<0.05 compared with the blank group. Notes: NC, negative control; miR-206, microRNA-206; ANXA2, Annexin A2.

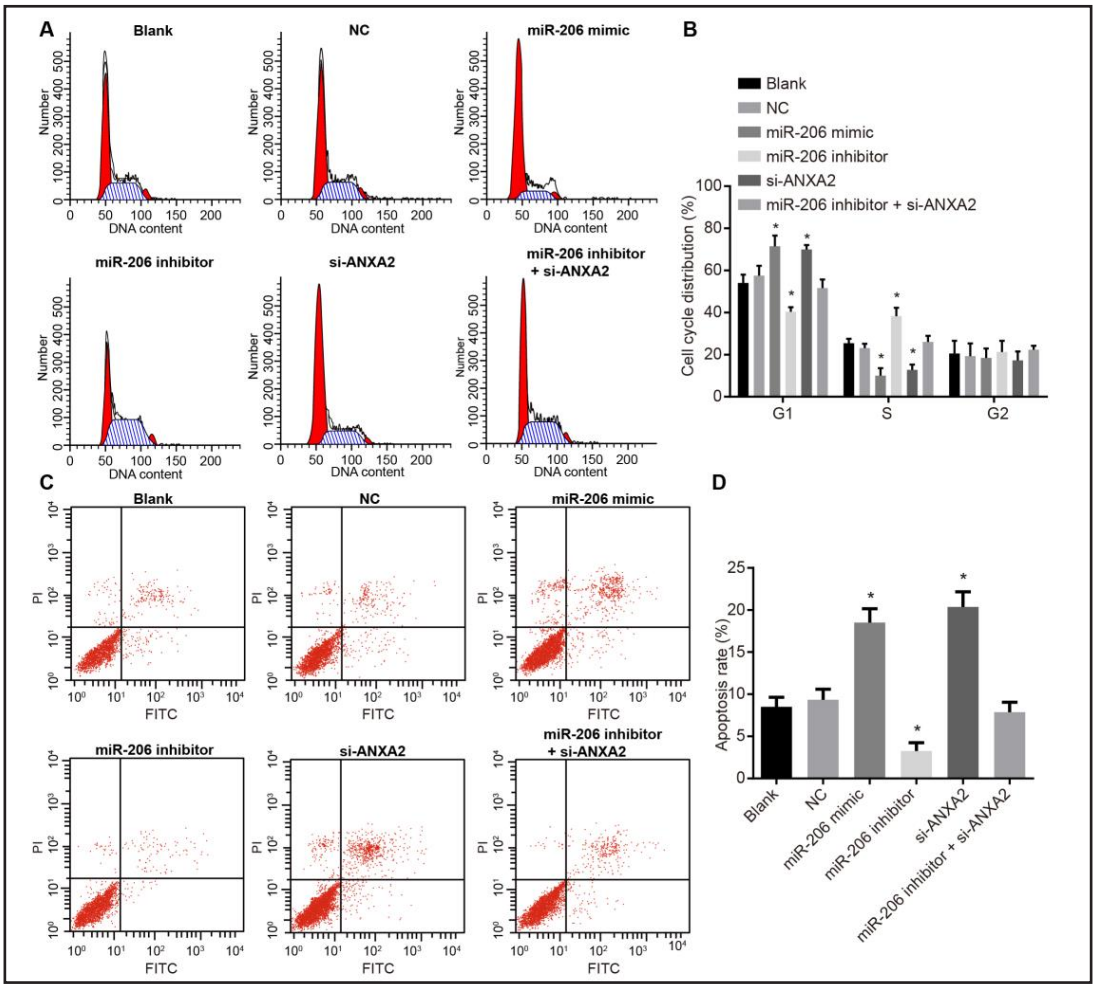

Fig. 7. Changes in cell apoptosis and cell cycle distribution in the six groups. Note: A, cell cycle distribution of the six groups; B, cartogram of cell cycle in the six groups; C, cell apoptosis analysis via flow cytometry; D, comparisons of apoptosis rate among the six groups; *, P<0.05 compared with the blank group. Notes: NC, negative control; miR-206, microRNA-206; ANXA2, Annexin A2.

and si-ANXA2 groups, but Bax expression increased (all $P < 0.05$). Taking the blank group as the control, reduced miR-206 expression was detected in the miR-206 inhibitor group, whereas the mRNA and protein expression of ANXA2, AKT, PAPP, FASN, Survivin, Mcl-1 and Bcl-2 was higher and Bax decreased (all $P < 0.05$). In the miR-206 inhibitor + si-ANXA2 group, the expression level of miR-206 was tested ($P < 0.05$), and the expression of miR-206, ANXA2, AKT, PAPP, FASN, Survivin, Mcl-1 and Bcl-2 at the mRNA and protein levels showed no statistically significant differences (all $P > 0.05$) (Fig. 5).

miR-206 overexpression inhibits OS cell proliferation

As shown in Fig. 6, no significant difference in cell growth was observed at each time point among the blank group, the NC group and the miR-206 inhibitor + si-ANXA2 group ($P >0.05$). Compared with the blank group, cell proliferation was inhibited in the miR-206 mimic and si-ANXA2 groups at all time points and was promoted in the miR-206 inhibitor group at all time points (all $P < 0.05$).

Comparisons of cell cycle distribution and apoptosis among the six groups after transfection

In the G1 and S phases, there was no notable difference in cell distribution among the blank group, the NC group and the miR-206 inhibitor + si-ANXA2 group ($P > 0.05$). Between

the miR-206 mimic group and the si-ANXA2 group, the cell distribution was also similar in the G1 and S phases (P > 0.05). Compared with the blank group, the miR-206 mimic group and the si-ANXA2 group had an increased cell number in G1 phase and a decreased cell number in S phase (P < 0.05), whereas the miR-206 inhibitor group had a decreased cell number in G1 phase but an increased number in S phase (P < 0.05).

No significant difference was observed in the cell apoptosis rate among the blank group, the NC group and the miR-206 inhibitor + si-ANXA2 group (P >0.05). There was also no significant difference in the cell apoptosis rate between the miR-206 mimic and the si-ANXA2 group (P > 0.05). Compared with the blank group, an increased cell apoptosis rate was observed in the miR-206 mimic group; however, the apoptosis rate in the miR-206 inhibitor group was reduced (all P < 0.05) (Fig. 7).

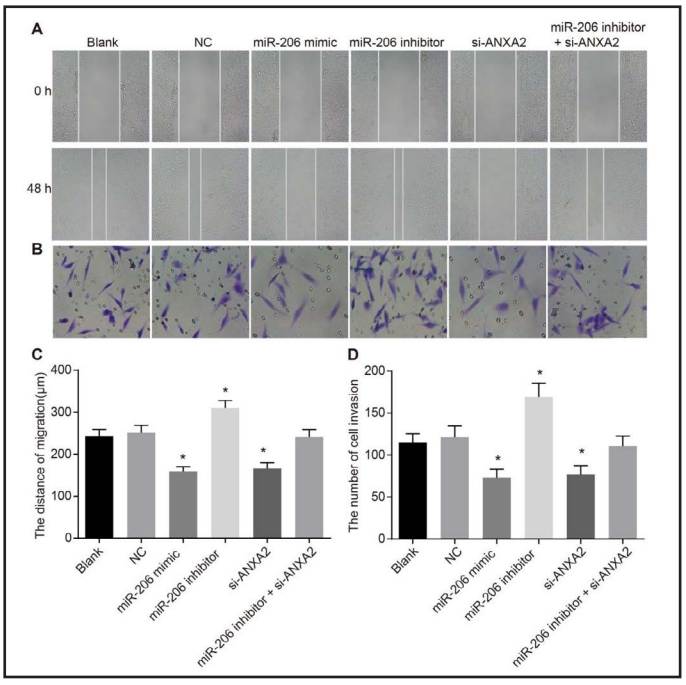

Fig. 8. Results of wound-healing and Transwell assays in each group. Note: A, microscopy images of the wound-healing assay at 0 h and 48 h (× 100); B, microscopy images of the Transwell assay (× 400); C, cell migration distance; D, the quantification of cell invasion from the upper chamber to the lower chamber; *, P<0.05 compared with the blank group. Notes: NC, negative control; miR-206, microRNA-206; ANXA2, Annexin A2.

miR-206 overexpression decreased migration intensity and invasive cell number

No notable differences in cell migration were detected among the blank group, the NC group and the miR-206 inhibitor + si-ANXA2 group or between the miR-206 mimic group and the si-ANXA2 group (P > 0.05). Compared with the blank group, the miR-206 mimic and si-ANXA2 groups had decreased migration intensity, but the miR-206 inhibitor group had increased migration intensity (all P < 0.05) (Fig. 8A).

The number of cells that invaded from the upper Transwell chamber to the lower chamber was similar among the blank group, the NC group and the miR-206 inhibitor + si-ANXA2 group, which resembled the comparison between the miR-206 group and the si-ANXA2 group (all P >0.05). Compared with the blank group, the number of cells invading from the upper chamber to the bottom chamber decreased largely in the miR-206 mimic group and the si-ANXA2 group but increased in the miR-206 inhibitor group (all P < 0.05) (Fig. 8B and C).

Discussion

A recent study showed that OS is the primary cause of cancer death in the second decade of life [1]. The introduction of traditional chemotherapy for OS, including key anticancer drugs, was popular 3 decades ago, but its further progress seems to have stagnated [14]. Emerging evidence has shown that miRNAs and the target genes that they regulate may offer new therapeutic targets against OS or be potential biomarkers [15]. The present study

focused on investigating the effects of miR-206 on regulating the proliferation and invasion of OS cells by targeting ANXA2 via the AKT signaling pathway. The results showed that miR-206 overexpression inhibited cell proliferation, migration and invasion and promoted apoptosis by inhibiting ANXA2 via the AKT signaling pathway.

Compared with osteochondroma tissues, the mRNA and protein expression of ANXA2, AKT, PARP, FASN, Survivin, Mcl-1, and Bcl-2 was strikingly increased, but that of Bax and miR-206 was decreased in OS tissues. Aberrant miR-206 expression has been predicted to be significant in the progression of OS, the most well-known malignant tumor, and down-regulation of miR-206 expression was recently shown in OS patients to occur more frequently and lead to higher mortality rates [16]. A previous study demonstrated that ANAX2, a phospholipid-binging protein, is essential in accelerating cancer metastasis, is highly expressed in many tumor types and plays positive or negative roles in cell proliferation, migration and other cellular functions [17]. It also has been widely reported that the AKT signaling pathway is oncogenic in humans, and hyper activation of AKT signaling in OS has been observed [18]. In a previous study, evodiamine, a type of traditional Chinese medicine, was effective against OS by down-regulating Bcl-2 and Survivin expression and upregulating Bax expression [19]. Furthermore, FASN is considered a potential target for treating OS, based on its low expression demonstrated in a previous study [20]. The above evidence prompted the design of a deeper-reaching experiment to confirm some relationships and find feasible treatments.

In this study, we found markedly decreased mRNA and protein expression of ANXA2, AKT, PARP, FASN, Survivin, Mcl-1 and Bcl-2 and increased expression of Bax in the miR-206 mimic and the si-ANXA2 groups compared with those in the blank group. In addition, ANXA2 was identified as the direct target gene of miR-206. A previous study also indicated that the ANXA2 gene is directly targeted by miR-206 in pancreatic adenocarcinoma cells, from which the inverse correlation between ANXA2 and miR-206 expression was evidenced [21]. It has been demonstrated that some miRNAs down-regulate AKT [22]; in particular, upregulation of miR-206 via transfection with a mimic significantly reduced AKT expression, indicating that miR-206 is an inhibitor of the AKT signaling pathway, consistent with our findings [23]. Mcl-1, a member of the Bcl-2 family that regulates cell processes, such as apoptosis, functions similarly to the Bcl-2 protein [24]. In addition, low expression of ANXA2 induced by ANXA2 siRNA reduced the expression of Bcl-2 but elevated Bax expression in some cancer cells, such as gastric cancer cells, as noted in a previous study, which also noted inhibition of AKT pathway activation [25]. These findings may help build a potential approach for novel treatments for this disease by regulating miR-206 and its target genes.

We also observed that OS cell proliferation, migration and invasion were all weakened and that cell apoptosis was accelerated in the miR-206 mimic group and the si-ANXA2 group, suggesting that silencing miR-206 and ANXA2 was a defense against OS progression. A previous study found that miR-206 overexpression was a restrictive factor for skeletal muscle satellite cell proliferation and for cell invasion of pancreatic adenocarcinoma cell lines [21, 26]. Wang, et al. also revealed that miR-206 overexpression promoted neural cell apoptosis by regulating Otx2, one of its target genes [27]. Furthermore, cell migration is a crucial step in cancer metastasis, and a previous study revealed that upregulation of miR-206 in lung adenocarcinoma cells inhibits cell migration [28]. In line with our results, another study also demonstrated that miR-206 might play a key role in the pathogenesis and development of OS and may provide a potential target for gene therapy [9]. As shown here, miR-206 inversely regulated ANXA2, and the correlation between si-ANXA2 treatment and cell functions may consistently increase. These findings shed light on the role of increased miR-206 expression in malignant progression of OS.

Collectively, our study showed that miR-206 overexpression blocks AKT signaling by down-regulating ANXA2, thereby inhibiting cell proliferation and invasion. This finding is a significant stride toward developing a novel therapy for OS. However, a more comprehensive study is urgently needed to determine the complexity of the genetic family and to fully explore its relationships.

Acknowledgements

We acknowledge the reviewers for their helpful comments on this paper.

Disclosure Statement

No conflict of interests exists.

References

1 Jones KB, Salah Z, Del Mare S, Galasso M, Gaudio E, Nuovo GJ, Lovat F, LeBlanc K, Palatini J, Randall RL, Volinia S, Stein GS, Croce CM, Lian JB, Aqeilan RI: miRNA signatures associate with pathogenesis and progression of osteosarcoma. Cancer Res 2012;72:1865-1877.
2 Bilbao-Aldaiturriaga N, Askaiturrieta Z, Granado-Tajada I, Goricar K, Dolzan V, For The Slovenian Osteosarcoma Study G, Garcia-Miguel P, Garcia de Andoin N, Martin-Guerrero I, Garcia-Orad A: A systematic review and meta-analysis of MDM2 polymorphisms in osteosarcoma susceptibility. Pediatr Res 2016;80:472-479.
3 Luetke A, Meyers PA, Lewis I, Juergens H: Osteosarcoma treatment - where do we stand? A state of the art review. Cancer Treat Rev 2014;40:523-532.
4 Huang J, Ni J, Liu K, Yu Y, Xie M, Kang R, Vernon P, Cao L, Tang D: HMGB1 promotes drug resistance in osteosarcoma. Cancer Res 2012;72:230-238.
5 Yan K, Gao J, Yang T, Ma Q, Qiu X, Fan Q, Ma B: MicroRNA-34a inhibits the proliferation and metastasis of osteosarcoma cells both *in vitro* and *in vivo*. PLoS One 2012;7:e33778.
6 Thayanithy V, Sarver AL, Kartha RV, Li L, Angstadt AY, Breen M, Steer CJ, Modiano JF, Subramanian S: Perturbation of 14q32 miRNAs-cMYC gene network in osteosarcoma. Bone 2012;50:171-181.
7 Kobayashi E, Hornicek FJ, Duan Z: MicroRNA Involvement in Osteosarcoma. Sarcoma 2012;2012:359739.
8 Kavitha N, Vijayarathna S, Jothy SL, Oon CE, Chen Y, Kanwar JR, Sasidharan S: MicroRNAs: biogenesis, roles for carcinogenesis and as potential biomarkers for cancer diagnosis and prognosis. Asian Pac J Cancer Prev 2014;15:7489-7497.
9 Bao YP, Yi Y, Peng LL, Fang J, Liu KB, Li WZ, Luo HS: Roles of microRNA-206 in osteosarcoma pathogenesis and progression. Asian Pac J Cancer Prev 2013;14:3751-3755.
10 Zhang X, Liu S, Guo C, Zong J, Sun MZ: The association of annexin A2 and cancers. Clin Transl Oncol 2012;14:634-640.
11 Bauerfeld CP, Rastogi R, Pirockinaite G, Lee I, Huttemann M, Monks B, Birnbaum MJ, Franchi L, Nunez G, Samavati L: TLR4-mediated AKT activation is MyD88/TRIF dependent and critical for induction of oxidative phosphorylation and mitochondrial transcription factor A in murine macrophages. J Immunol 2012;188:2847-2857.
12 Fu X, Tian J, Zhang L, Chen Y, Hao Q: Involvement of microRNA-93, a new regulator of PTEN/Akt signaling pathway, in regulation of chemotherapeutic drug cisplatin chemosensitivity in ovarian cancer cells. FEBS Lett 2012;586:1279-1286.
13 Ayuk SM, Abrahamse H, Houreld NN: The role of photobiomodulation on gene expression of cell adhesion molecules in diabetic wounded fibroblasts *in vitro*. J Photochem Photobiol B 2016;161:368-374.
14 Yamamoto N, Tsuchiya H: Chemotherapy for osteosarcoma - where does it come from? What is it? Where is it going? Expert Opin Pharmacother 2013;14:2183-2193.
15 Namlos HM, Meza-Zepeda LA, Baroy T, Ostensen IH, Kresse SH, Kuijjer ML, Serra M, Burger H, Cleton-Jansen AM, Myklebost O: Modulation of the osteosarcoma expression phenotype by microRNAs. PLoS One 2012;7:e48086.
16 Zhang C, Yao C, Li H, Wang G, He X: Serum levels of microRNA-133b and microRNA-206 expression predict prognosis in patients with osteosarcoma. Int J Clin Exp Pathol 2014;7:4194-4203.
17 Lokman NA, Ween MP, Oehler MK, Ricciardelli C: The role of annexin A2 in tumorigenesis and cancer progression. Cancer Microenviron 2011;4:199-208.

18 Zhang J, Yu XH, Yan YG, Wang C, Wang WJ: PI3K/Akt signaling in osteosarcoma. Clin Chim Acta 2015;444:182-192.
19 Bai X, Meng H, Ma L, Guo A: Inhibitory effects of evodiamine on human osteosarcoma cell proliferation and apoptosis. Oncol Lett 2015;9:801-805.
20 Yang YQ, Qi J, Xu JQ, Hao P: MicroRNA-142-3p, a novel target of tumor suppressor menin, inhibits osteosarcoma cell proliferation by down-regulation of FASN. Tumour Biol 2014;35:10287-10293.
21 Estrela S, Whiteley M, Brown SP: The demographic determinants of human microbiome health. Trends Microbiol 2015;23:134-141.
22 Sayed D, Abdellatif M: AKT-ing via microRNA. Cell Cycle 2010;9:3213-3217.
23 Chen QY, Jiao DM, Wang J, Hu H, Tang X, Chen J, Mou H, Lu W: miR-206 regulates cisplatin resistance and EMT in human lung adenocarcinoma cells partly by targeting MET. Oncotarget 2016;7:24510-24526.
24 Thomas LW, Lam C, Edwards SW: Mcl-1; the molecular regulation of protein function. FEBS Lett 2010;584:2981-2989.
25 Lin ZY, Huang YQ, Zhang YQ, Han ZD, He HC, Ling XH, Fu X, Dai QS, Cai C, Chen JH, Liang YX, Jiang FN, Zhong WD, Wang F, Wu CL: MicroRNA-224 inhibits progression of human prostate cancer by downregulating TRIB1. Int J Cancer 2014;135:541-550.
26 Chen JF, Tao Y, Li J, Deng Z, Yan Z, Xiao X, Wang DZ: microRNA-1 and microRNA-206 regulate skeletal muscle satellite cell proliferation and differentiation by repressing Pax7J Cell Biol 2010;190:867-879.
27 Wang R, Hu Y, Song G, Hao CJ, Cui Y, Xia HF, Ma X: MiR-206 regulates neural cells proliferation and apoptosis via Otx2. Cell Physiol Biochem 2012;29:381-390.
28 Chen X, Tong ZK, Zhou JY, Yao YK, Zhang SM, Zhou JY: MicroRNA-206 inhibits the viability and migration of human lung adenocarcinoma cells partly by targeting MET. Oncol Lett 2016;12:1171-1177.